https://rbgeomorfologia.org.br/
ISSN 2236-5664

Revista Brasileira de Geomorfologia

v. 26, nº 3 (2025)

http://dx.doi.org/10.20502/rbg.v26i3.2620

Research Article

Glacial geomorphological characterization and glacigenic sedimentation in Admiralty Bay, Maritime Antarctica

Caracterização geomorfológica glacial e sedimentação glacigênica na Baía do Almirantado, Antártica Marítima

Cleiva Perondi[1], Kátia Kellem da Rosa[2], Rosemary Vieira[3], Carina Petsch[4], Luiz Felipe Velho[5], Nicholas Becker Pires Pi[6], Sandra Bromberg[7] e Jefferson Cardia Simões[8]

[1] Universidade Federal do Rio Grande do Sul, Laboratório de Sedimentologia e geomorfologia glacial, Centro Polar e Climático, Porto Alegre, Brasil. E-mail: cleivaperondi@gmail.com.
ORCID: https://orcid.org/0000-0003-2202-2721

[2] Universidade Federal do Rio Grande do Sul, Laboratório de Sedimentologia e geomorfologia glacial, Centro Polar e Climático, Departamento de Geografia, Porto Alegre, Brasil. E-mail: katia.rosa@ufrgs.br.
ORCID: https://orcid.org/0000-0003-0977-9658

[3] Universidade Federal Fluminense, Instituto de Geociências, Niterói, Brasil. E-mail: rosemaryvieira@id.uff.br.
ORCID: https://orcid.org/0000-0003-0312-2890

[4] Universidade Federal de Santa Maria, Departamento de Geociências, Porto Alegre, Brasil. E-mail: carina.petsch@ufsm.br.
ORCID: https://orcid.org/0000-0002-1079-0080

[5] Instituto Federal de Educação, Ciência e Tecnologia do Rio Grande do Sul, Porto Alegre, Brasil. E-mail: luiz.velho@poa.ifrs.edu.br.
ORCID: https://orcid.org/0000-0001-9543-7544

[6] Universidade Federal do Rio Grande do Sul, Laboratório de Sedimentologia e geomorfologia glacial, Centro Polar e Climático, Porto Alegre, Brasil. E-mail: nickbpy@gmail.com.
ORCID: https://orcid.org/0009-0006-5068-2267

[7] Universidade de São Paulo, Departamento de Oceanografia Biológica, Instituto Oceanográfico, São Paulo, Brasil. E-mail: bromberg@usp.br.
ORCID: https://orcid.org/0000-0003-2159-5683

[8] Universidade Federal do Rio Grande do Sul, Centro Polar e Climático, Departamento de Geografia, Porto Alegre, Brasil. E-mail: jefferson.simoes@ufrgs.br.
ORCID: https://orcid.org/0000-0001-5555-3401

Received: 23/09/2024; Accepted: 09/07/2025; Published: 14/07/2025

Abstract: The study of the relationship between geomorphology and sedimentation processes is important as it clarifies information about relict landscapes. These processes are understood based on glacial landforms and the characteristics of their sediments. The objective of this article is to investigate glacial geomorphology and associate it with the attributes of glaciogenic sediments in the proglacial areas of the Baranowski, Windy, and Dobrowolski glaciers in Admiralty Bay, King George Island, and to infer changes in these glacial environments. Sediment samples were collected from depositional features during fieldworks (2019 and 2023), which underwent granulometric and morphoscopic analyses. The visual identification of glacial landforms followed criteria of morphology, morphometric characteristics, depositional environment, sedimentology and genesis. The sediments were interpreted as glaciogenic and related to moraine deposits. The geomorphological mapping identified glacial landforms that provide information on aspects such as the direction of glacial flow, area, and thermo-basal regime. The subaerial environment was observed to be related to the submarine environment through glaciers, mass movements and the sediment supply via meltwater. Thus, there is continuity in the processes related to the glacier: the closer

to it, the more dynamic the environment, while as the distance increases, the terrain tends to present reworked or smoothed landforms.

Keywords: Glacial landforms; Glacial retreat; King George Islands; Moraine ridge; Sediment-form association.

Resumo: O estudo da relação entre a Geomorfologia e processos de sedimentação são importantes, pois, esclarecem informações sobre paisagens relictuais. Esses processos são compreendidos com base nas formas de relevo glaciais e nas características dos seus sedimentos. O objetivo da pesquisa é interpretar as formas de relevo deposicionais glaciais em áreas proglaciais da Baía do Almirantado através de mapeamento geomorfológico elaborado a partir de 9 amostras sedimentológicas e de interpretação de imagens orbitais. Foram coletadas amostras sedimentares de feições deposicionais em trabalho de campo realizado em 2019, que passaram por análises granulométricas e morfoscópicas. A identificação visual das formas de relevo glaciais seguiu critérios como que envolvem a morfologia, a morfometrica, o ambiente deposicional, a sedimentologia e a gênese. Os sedimentos foram interpretados como glacigênicos, relacionados a depósitos morâinicos. O mapeamento geomorfológico identificou as formas de relevo glaciais que permitiram compreender sobre os aspectos de direção do fluxo glacial, área da geleira e regime termo-basal. Observou-se que o ambiente subaéreo apresenta relação com o ambiente submarino através de movimentos de massa e do aporte sedimentar a partir da água de degelo. Dessa forma, há continuidade nos processos relacionados à geleira: quanto mais próximo a ela, mais dinâmico o ambiente, enquanto ao se distanciar o terreno tende a apresentar formas de relevo retrabalhadas ou suavizadas.

Palavras-chave: Formas glaciais, Cristas morâinicas; Retração glacial; Associação forma-sedimento; ilha Rei George.

1. Introduction

The cryosphere is a crucial component of the global climate system (DING et al., 2021). Glacial ice—including ice sheets and ice caps—covers approximately 10% of the Earth's surface and stores 69% of the planet's freshwater (SHAHGEDANOVA, 2021). However, due to atmospheric warming, glaciers in various regions of the world have shown a negative mass balance, leading to a reduction in global ice volume (HOCK and HUSS, 2021).

In the southern polar region, the Antarctic Peninsula (AP) has shown consistent records of rising atmospheric temperatures since the mid-20th century (TURNER et al., 2016; SIEGERT et al., 2019). In early February 2020, the AP and its surrounding islands experienced one of the most intense heatwaves ever recorded since the onset of reliable observations (BARRIOPEDRO et al., 2022). As a result of this atmospheric warming, multiple studies have reported the continuous retreat of glaciers on King George Island (KGI) since the second half of the 20th century (KEJNA, ARAZNY, SOBOTA, 2013; PERONDI, ROSA, VIEIRA, 2019; ROSA et al., 2020), where the study area of this research is located.

Glacier retreat exposes ice-free areas that are susceptible to rapid change due to the presence of meltwater and sediments (BALLANTYNE, 2002), as well as the exposure of subglacial terrain (DIOLAIUTI; SMIRAGLIA, 2010; SIEGERT et al., 2010). In this context, terrestrial glacial geomorphological records provide valuable information on glacier extent, thickness, timing of glaciation and deglaciation (SUGDEN et al., 2006), as well as on flow direction, flow patterns, and thermal regimes (BENNET; GLASSER, 1996; NAPIERALSKI et al., 2007).

Subglacial erosion processes are complex, influenced by bedrock characteristics, glacial dynamics, friction, and lubrication at the ice-rock interface (DREWRY, 1986). These processes—erosion, deposition, transport types, and thermal basal regimes—are interpreted through landforms and the sediments that compose them. In the case of sediments, characteristics such as grain texture and morphology are especially informative (BENNET; GLASSER, 1996). Thus, the sedimentological properties of landforms in glacial environments offer insights into their origin and evolution (KNIGHT et al., 2000).

Regarding the study area, several investigations have focused on sedimentary analysis of geomorphological features in the ice-free zones of Admiralty Bay, KGI. Rosa et al. (2011) mapped depositional and erosional landforms in the ice-free area of Wanda Glacier through field surveys, sedimentological analyses, and satellite image interpretation, identifying glacier retreat based on the location of moraine ridges. In Martel Inlet, the ice-free areas near Dobrowolski Glacier were studied by Perondi et al. (2023) using bathymetric data and satellite imagery. This research identified smaller, more recent moraine banks dated from the mid-20th century to recent decades, as well as a prominent, older moraine bank associated with the Little Ice Age (approximately 1550 to 1800).

The modern depositional environments of the Ecology, Baranowski, and Windy Glaciers, located on the western coast of Admiralty Bay, were studied by Perondi et al. (2019), who carried out a geomorphological mapping of mesoscale depositional features. The authors identified the retreat of the glaciers based on the presence of lateral moraines, recessional frontal moraines, latero-frontal moraines, eskers, and water bodies such as lakes, lagoons, and drainage channels. The Windy Glacier was studied by Kreczmer et al. (2021), who reported the presence of features such as flutings, drumlins, and other depositional landforms in the ice-free area.

To understand the evolution of the subaerial landscape, as well as to contextualize the dynamics of glacial advance and retreat, it is important to spatially delineate the main subglacial and ice-margin geomorphological features. Thus, the objective of this research is to interpret glacial depositional landforms in the proglacial areas of Admiralty Bay through geomorphological mapping based on sedimentological analyses and the interpretation of orbital images and digital elevation models.

2. Study area

The IRG (Figure 1B) is the largest island in the South Shetland archipelago. It has an area of 1250 km², with a distance of 80 km along its central axis in the southwest-northeast direction and is approximately 15 km wide. The IRG has 70 drainage basins (BREMER, 1998), and its ice cap has a maximum altitude of approximately 720 m (RÜCKAMP et al., 2011). To the north, the IRG reaches the Drake Passage, and, to the south, it is separated from the PA by the Bransfield Strait (BIRKENMAJER, 1980) (Figure 1A).

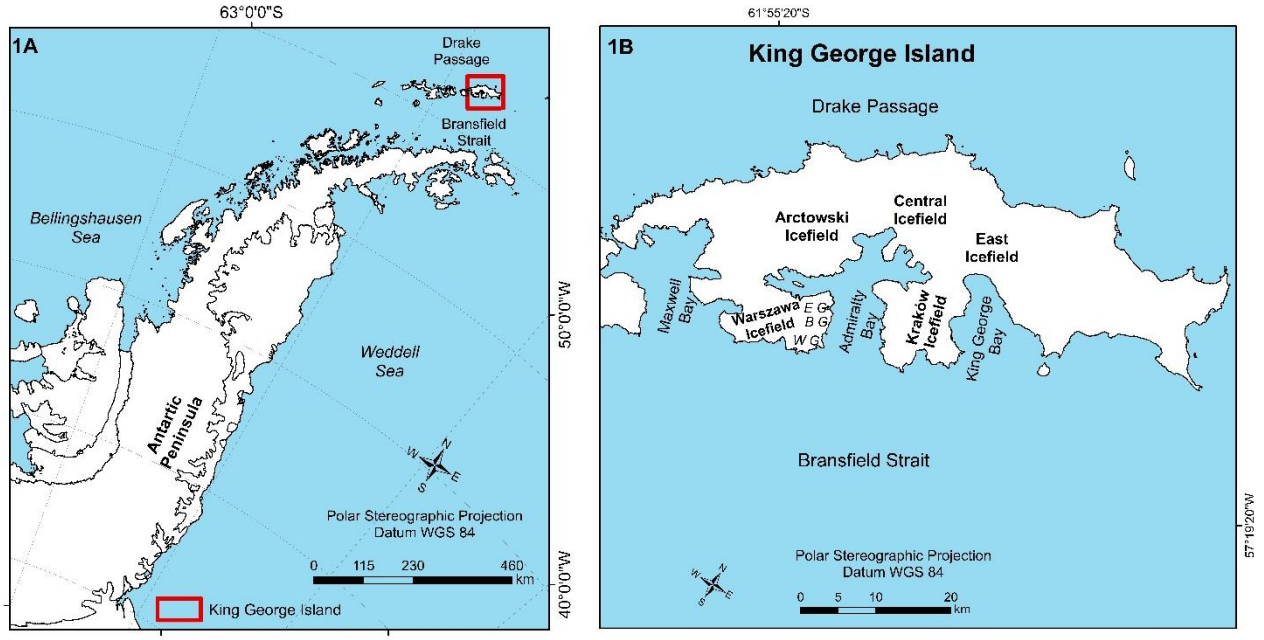

Figure 1. Location map of the study area. CG: Ice field, EG: Ecology Glacier, BG: Baranowski Glacier, WG: Windy Glacier. Source: Quantarctica (MATSUOKA et al., 2018).

The IRG is covered by an ice cap divided into domes connected by drainage basins that flow towards the glaciomarine environment (BREMER; ARIGONY-NETO; SIMÕES, 2004). The BA fjord, located on the southern coast of the IRG (Figure 1B), is elongated, approximately 16 km long and 6 km wide at its narrowest point. It has steep walls and a U-shaped valley and can reach depths of up to 510 m (MAGRANI, 2014).

The IRG is located in the centre of the magmatic arc of the South Shetland Islands (KRAUS; POBLETE; ARRIAGADA, 2010), and was subject to Cenozoic structural deformation, linked to tectonic movements of the plate along the margin of the Pacific Ocean, which resulted in the formation of faults in different directions (TOKARSKI, 1987). Two significant faults are recorded, with an ENE-WSW orientation: the Ezcurra Fault (EF) and the Collins Fault (TOKARSKI, 1987). These faults influence the shape of the islands and are reflected in the location and orientation of bays and inlets (KRAUS; POBLETE; ARRIAGADA, 2010). Because it is primarily covered by ice, the IRG reduces the action of geological processes on the surface. It restricts them mainly to the coastal area, on the

margins of glaciers and nunataks. Due to the isostatic elevation due to deglaciation in the last 10 thousand years, recent rocky beaches and coasts with sediments vary between sand and gravel (BIRKENMAJER, 1980).

The average annual temperature for the IRG is -2.8°C, for the winter months (June, July and August), with a minimum temperature of -15.5°C and a maximum of -1.0°C. In the summer (December, January and February) the temperature varies between -1.3°C (minimum) and 2.7°C (maximum) (FERRON et al., 2004). Cyclones influence the area's climate with an east-west orientation around the Antarctic continent, which provides conditions for rain, drizzle and snow in the summer months. However, cyclones in the Weddell Sea region bring cold air, snow and low temperatures to the IRG (SETZER et al., 2004).

Adjacent to the fjord, tidewater glaciers and glaciers end on land. Tidewater glaciers present iceberg calving or growlers (SILVA; ARIGONY-NETO; BICCA, 2019). Approximately 10% of the total surface area of the IRG is ice-free (138 km2) (DĄBSKI et al., 2020). As a response of glaciers to climate variations, there are ice-free areas with exposed relief features, such as moraine ridges, flutings, eskers, meltwater channels and lakes (PERONDI; ROSA; VIEIRA, 2019). The IRG has 144 lakes, distributed in the island's southern, eastern, southwestern, southeastern, and western portions (OLIVEIRA, 2020).

3. Materials and methods

3.1. Sedimentary samples

Nine sediment samples were collected during OPERANTAR (Antarctic Operation) XXXVIII 2019/2020 in proglacial areas of the Windy and Baranowski glaciers (Table 1). Sediments were collected at a depth of 3 cm. The material collected with a shovel was packed in plastic bags. At each collection point, geographic coordinates were recorded using a GNSS (Global Navigation Satellite System).

In the glacier-free area of the Windy Glacier, two samples are located 1 m from the glacier ice margin, while the other samples are 290 m and 380 m away. Regarding the ice-free area of the Baranowski glacier, two samples are in contact with the glacier front; two samples are about 1 m from the glacier front; and one sample is located 40 m away from the glacier front (Figure 2).

Table 1. Location and characterization of samples. The sediment samples collected in the proglacial area of the Baranowski Glacier are 1, 6, 7, 8, and 9, and those from Windy Glacier are 2, 3, 4, and 5.

Sample	Geographical Coordinates	Altitude WGS84 (m)	Ice margin distance (m)
8	62°11’55.9” S, 58°26’56.7” W	1	1
9	62°11’57.2” S, 58°26’54.4” W	1	1
7	62°11’58.7” S, 58°26’53.7” W	1	In contact with the glacier
6	62°11’58.7” S, 58°26’53.7” W	1	In contact with the glacier
1	62°11’53.5” S, 58°26’56.7 W	22	40
2	62°13’44.5”S, 58°28’49.0”W	15	1
3	62°13’43.8”S, 58°28’02.0”W	8	290
4	62°13’41.0”S, 58°28’21.3”W	16	1
5	62°13’49.5”S, 58°28’04.6”W	47	380

Source: Perondi et al. (2025).

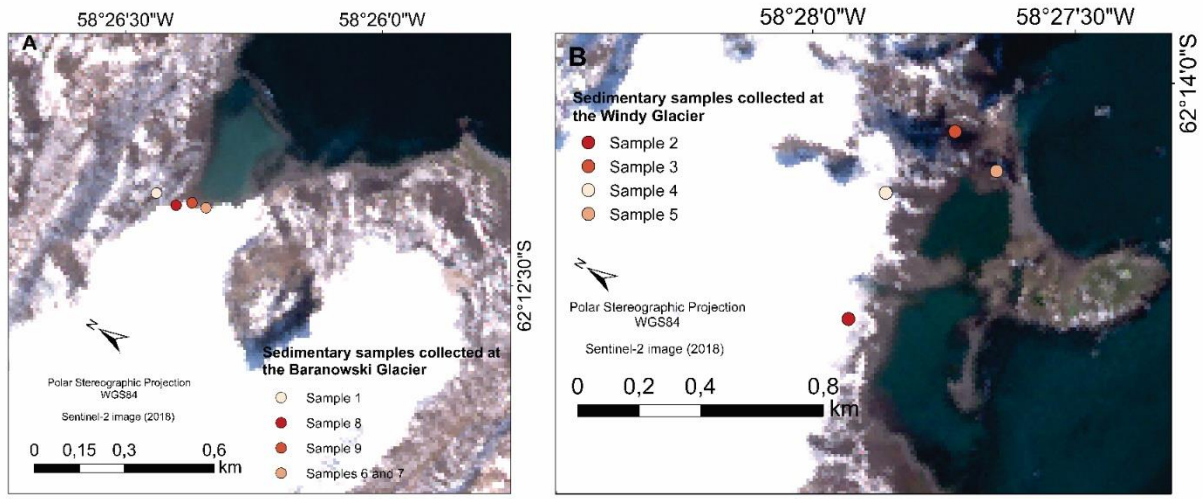

Figure 2. Sample locations. Figure A – Baranowski Glacier; Figure B – Windy Glacier.

3.2 Laboratory Analyses

Sediment analyses were carried out at the Physical Geography Laboratory of the Department of Geography and at the Coastal and Oceanic Geology Study Center (CECO) of UFRGS. The following analyses were performed: (i) grain size analysis; and (ii) morphoscopic analysis.

3.2.1 Grain Size Analysis

In the laboratory, the collected material was passed through a 0.064 mm mesh sieve to distinguish sediment grain sizes as "coarse" and "fine" (WENTWORTH, 1922). Sediments larger than 0.064 mm were further separated using a series of sieves with decreasing mesh sizes (16 mm to 0.064 mm), followed by weighing according to textural classes (sand, granule, pebble, and cobble). The silt and clay fractions were separated using the pipette method, based on Stokes' Law.

Grain sorting was assessed according to Folk and Ward's (1957) method, which provides statistical parameters such as mean, skewness, and kurtosis. Ternary diagrams were created to represent each sample's grain size distribution, indicating whether the distribution is unimodal, bimodal, or multimodal.

3.2.2 Morphoscopical Analysis

Morphoscopical analysis was conducted on sediment grains larger than 1 mm, with 50 grains analyzed from each class. The axes of the grains were measured using a calliper and a trinocular microscope. One of the indices used was the C_{40}, representing the number of sediment grains in a sample with a c/a axis ratio (Figure 3) less than or equal to 0.4 (HANÁČEK et al., 2013).

This index differentiates subglacially transported sediments (low C_{40} values) from supraglacially transported ones (high C_{40} values) within the glacier (BENNET et al., 1997). The results were plotted using the Tri-Plot software. Clast shape was defined based on the relationship between the three orthogonal axes: a (longest), b (intermediate), and c (shortest) (HUBBARD; GLASSER, 2005). Histogram charts were created in Excel for each sample to analyze grain roundness and quantify the occurrence of striations.

The RA index was also calculated to indicate the percentage of grain roundness, categorized as: VA – very angular; A – angular; SR – sub-rounded; R – rounded; and WR – well-rounded. Roundness analysis followed Krumbein's method (1941), applying his classification chart (ROSA, 2008).

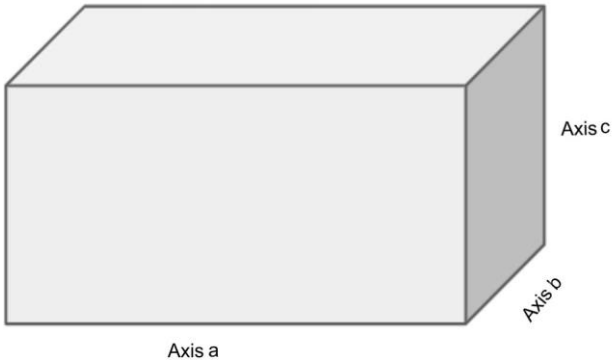

Figure 3. The *a* axis is the longest axis of a particle, the *b* axis is the intermediate axis, and the *c* axis is the shortest axis. Source: Hubbard; Glasser (2005).

3.3 Geomorphological Mapping

The geomorphological mapping of the subaerial sector was carried out through the interpretation of the following co-registered geospatial data: Tandem-X Digital Elevation Model (TanDEM-X, 2025), Antarctic Reference Elevation Model (REMA) (HOWAT et al., 2022), Sentinel-2 (2018 and 2020), WorldView-2 (2014), and PlanetScope (2019); in addition to the results obtained from the granulometric and morphoscopic analyses detailed in the previous section. Furthermore, the glacial landform mappings by Perondi, Rosa, and Vieira (2019) for the western margin of Admiralty Bay were reviewed. The identification of glacial relief features was conducted manually using ArcGIS. The methodology was based on identification criteria proposed by Bennet and Glasser (1996), Ottesen and Dowdeswell (2006), Benn and Evans (2010), Streuff et al. (2015), and Wölfl et al. (2016).

The interpretation methodology involved aspects such as morphology, morphometric characteristics, depositional environment, sedimentology, genesis, and context about the glacier, either parallel or perpendicular to the ice flow (Table 2). The satellite image identified each relief feature based on a visual identification criterion. The results were compared with those from the sedimentary analyses. Moraines were compared within each depositional environment according to the degree of spacing between the ridges. Linear features were interpreted and classified according to the presence or absence of stoss-and-lee blocks in the WorldView-2 image (2014) visualization. The landform received classification in the attribute table of the shapefile in ArcGIS according to Table 2.

4. Results

4.1. Sedimentary interpretation

Samples 1, 6, 7, 8, and 9 were collected in the glacier-free area of the Baranowski Glacier. Sample 1 (Figure 4A) was collected on an elongated relief feature located near and with a configuration parallel to the Baranowski Glacier margin (approximately 22 m away). It is predominantly composed of gravel and very coarse sand (Table 3), poorly sorted, with a polymodal distribution and low C_{40} index (10%) (Figure 8).

Sample 6 is classified as very fine-gravelly sand and very poorly sorted. It is composed of 28% gravel, 54% sand, 6% silt, and 12% clay (Table 3). It has a low C_{40} index (16%) and a polymodal granulometric distribution (Figure 6). Sample 7 contains fine sandy gravel (Table 3) and is poorly sorted. It is composed of sand and gravel. It has a low C_{40} index (12%) (Figure 8) and a polymodal granulometric distribution (Figure 6). This sedimentary sample was collected at the ice-bedrock interface at the current front of the Baranowski Glacier. Sample 8, collected laterally to the Baranowski Glacier (Figures 2 and 5B), is classified as fine sandy gravel and poorly sorted, with a polymodal distribution characteristic of subglacial transport. Its C_{40} index (18%) is low. It is composed of 54% gravel and 46% sand (Table 3).

Sample 9 (Figure 2) is classified as very fine sandy gravel and poorly sorted. Its granulometric distribution is polymodal. It has a low C_{40} index (18%) (Figures 8 and 9). It is composed of 67% sand and 33% gravel (Table 3).

This sample was collected at the front of the Baranowski Glacier, perpendicular to the glacial flow and near a meltwater channel.

Table 2. Criteria for identifying depositional and erosive landforms in subaerial glacial environments.

Landform	Depositional Environment	Genetic Processes[1]	Sediment/Form Association	Field or Satellite Image Identification Criteria	Relevance[1]
Advance frontal moraine	Maximum glacier advance limit	Formed by sediment deposition through mass movement and glaciotectonic activity	Coarse-grained sediments with rounded, faceted, striated clasts deposited directly by glacial action	Rough texture; composed of arcuate ridges; may be poorly preserved; reflect the former glacier margin; located near and transverse to the current glacier front	Records stationary glacial stages
Recessional frontal moraine	Glacier front margin	Formed during stabilization of the glacier front during retreat; pushed or deposited by minor readvances	Till of coarse and poorly sorted grains; characteristics vary depending on active or passive transport	Rough texture; transverse to ice flow; may appear as low ridges, linear belts, or discontinuous mounds	Records temporary glacier stability during advance or retreat
Push moraine	Parallel to glacier margins	Sediments are pushed during winter readvances and glacial stabilizations	Can be composed of subglacial deposits laid down in summer and pushed in winter	Rough texture; irregular and sinuous in shape; rarely more than 1 m high; elevated ridges transverse to the glacier front	Indicates annual glacial advance during winter
Esker	In contact with glacier	Formed by subglacial meltwater streams filling ice-bed channels with sediments	Mixed grain sizes, generally coarse; gravel and glaciofluvial sand with rounded grains due to meltwater transport	Rough texture; typically isolated; individual sinuous ridges with gentle slopes in longitudinal profile; aligned with former subglacial drainage	Indicates subglacial channel flow, wet-based thermal regime, and direction of ice flow
Meltwater channel	With or without direct glacier contact	Formed by fluvial meltwater discharge	Coarser sediments; detritus reflects transport by meltwater	Finer texture; darker tones in false-color composites using near-infrared; typically appear as braided channels	Indicates glacier advance and retreat dynamics

[1]Informations according to Sugden; John (1984), Hambrey (1994), Bennet; Glasser (1996), Brennand (2004), Assine; Vesely (2008), Benn; Evans (2010), Dąbski (2020).

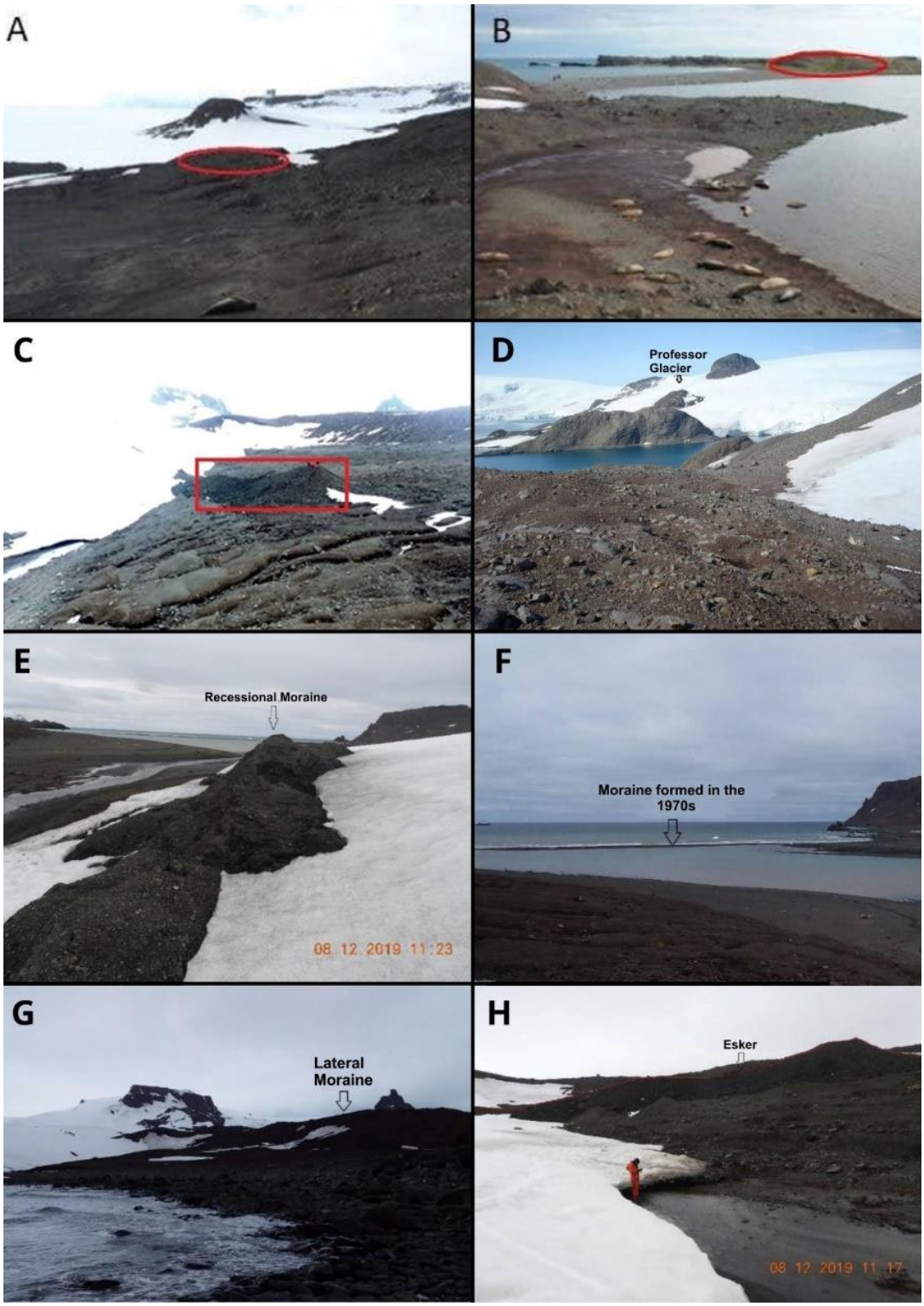

Figure 4. Representation of sampling sites and landforms in the study area. (A) Location of Sample 4; (B) sample at the front of Windy Glacier; (C) indicates the sampling location of Sample 1; (D) lateral scarp of Professor Glacier with a view toward Dobrowolski Glacier; (E) shows the recessional moraine of Baranowski Glacier; (F) displays the latero-frontal moraine damming the lagoon in front of Baranowski Glacier; (G) shows the lateral moraine of Baranowski Glacier; and (H) presents an esker adjacent to Baranowski Glacier. Source: Photographs by Cleiva Perondi (2019) and Rosemary Vieira (2019).

Table 3. Characteristics of the sediment samples analyzed. Samples 2, 3, 4, and 5 are from Windy Glacier, and samples 1, 6, 7, 8, and 9 are from Baranowski Glacier.

Sample	Gravel (granule to boulder) (%)	Sand (%)	Silt and clay (%)	Textural class (Folk; Ward, 1957)
1	60	40	0	Very coarse sand
2	28	71	1	Very coarse sand
3	22	76	2	Very coarse sand with fine gravel
4	38	59	3	Coarse sandy gravel
5	68	32	0	Very fine sandy gravel
6	28	54	18	Very fine sandy gravel with silt
7	48	52	0	Fine sandy gravel
8	54	46	0	Fine sandy gravel
9	33	67	0	Very fine sandy gravel

Samples 2, 3, 4, and 5 were collected at the front of Windy Glacier. Sample 2 (Figure 2) is classified as very coarse, poorly sorted sand. It shows a low C_{40} index (32%) and a polymodal grain size distribution. The sample is composed of sand and gravel—71% and 28%, respectively—with smaller amounts of silt and clay (Table 3). It was collected adjacent to the Windy Glacier front, in a deposit spatially arranged perpendicular to the glacier margin.

Sample 3 (Figures 2 and 4B) consists of very coarse, fine gravelly sand and poorly sorted. Its grain size distribution is polymodal, and it has a low C_{40} index (24%) (Figure 9). It comprises 76% sand and 22% gravel, with minor proportions of silt and clay (Table 3). The location where Sample 3 was collected represents a deposit with a spatial arrangement parallel and lateral to Windy Glacier (Figure 5B).

Sample 4 (Figures 2 and 4A) is classified as coarse sandy gravel and is very poorly sorted, with a low C_{40} index (20%). It was collected at the frontal zone of the Windy Glacier, in a spatial arrangement parallel to the glacier margin. Its composition is mainly sand (59%), with smaller amounts of gravel, silt, and clay (Table 3). Sample 5 (Figures 2 and 4B) is characterized as very fine sandy gravel, poorly sorted, and with a polymodal grain size distribution (Figure 6).

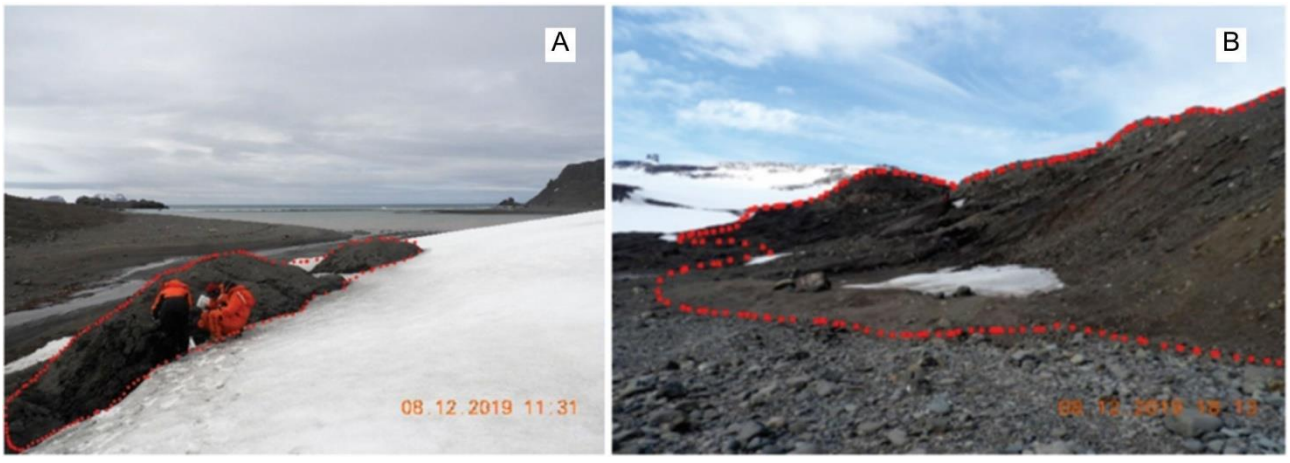

Figure 5. A – Sampling site of Sample 8; B – Sample 3 in the proglacial environment. The red dotted lines indicate the landforms where the sediment samples were collected. Photographs by Rosemary Vieira (2019).

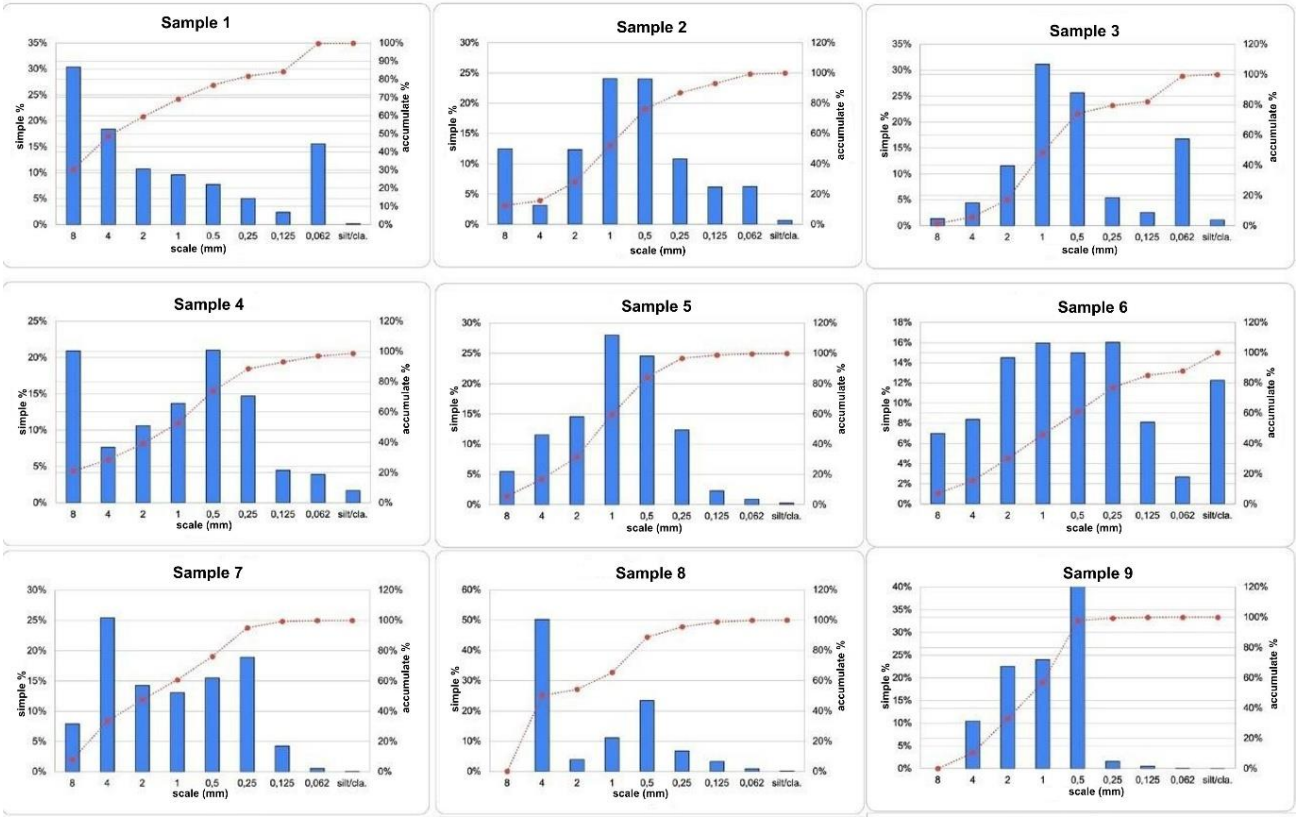

Figure 6. Grain size distribution graph for each collected sediment sample. The simple absolute frequency is in percentual values.

The sample 5 is predominantly composed of gravel (68%) and has a low C_{40} index (22) (Figure 8 and 9). This sample was collected approximately 380 meters from the current glacier front. The sedimentary characteristics of these samples (4 and 5) indicate direct glacial influence and reflect dynamic depositional processes in the proglacial environment of the Windy Glacier. The sediment samples from the ice-free area of the Windy Glacier are predominantly composed of very coarse sand in two cases and coarse sandy gravel in the other two.

All samples, except for sample 8, contain striated grains, with sample 6 showing the highest proportion of striations (18%) (Figure 7). The ternary diagrams (Figure 9) reveal a high proportion of grains with a c:a ratio below 0.4 across all samples. These diagrams place the samples in the upper region of the ternary plot, indicating spherical grain shapes.

The covariance diagrams between the RA and C_{40} indices (following Benn and Ballantyne, 1994; Figure 8) show that sample 7 exhibits an intermediate percentage of angular grains and elongated or flattened clasts (intermediate RA values and high C_{40}), distinguishing it from the other samples (1–6, 8–9), which have a lower percentage of angular grains and elongated or flattened clasts (low to medium RA and low C_{40} values) (Figure 8).

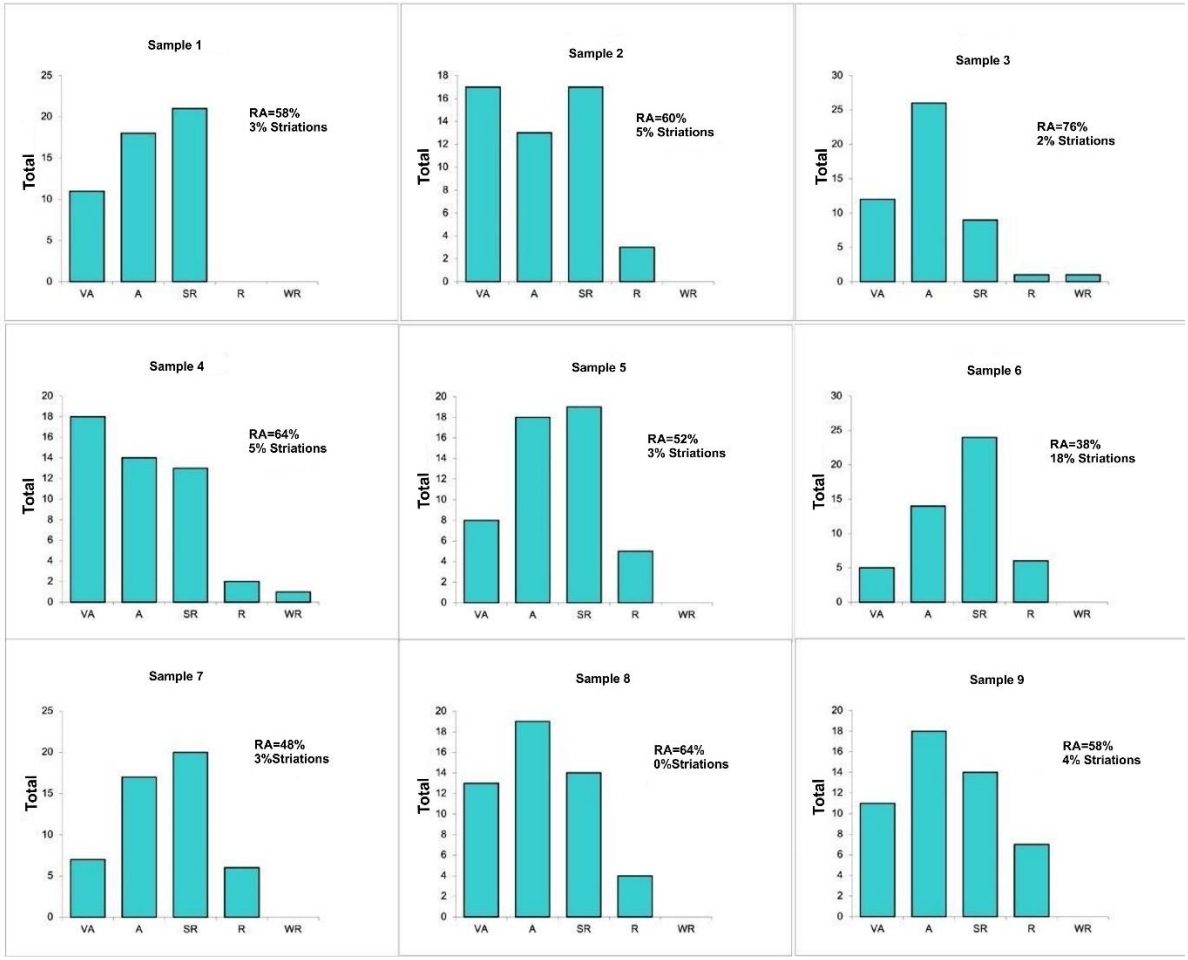

Figure 7. Grain shape characteristics for each collected sample. VA: very angular, A: angular, SR: sub rounded, R: rounded and WR: Well rounded. RA: índice percentual dos grãos angulosos.

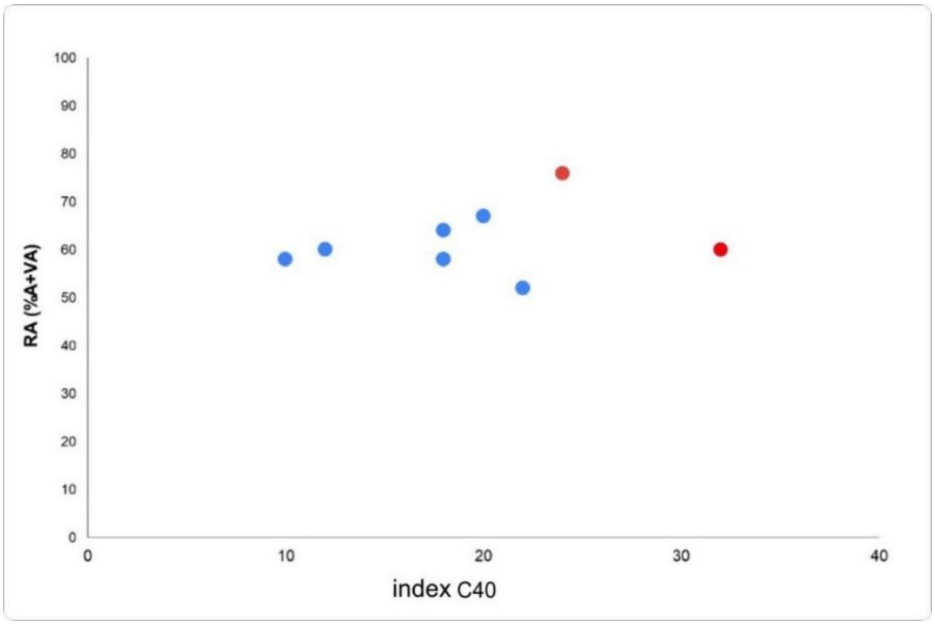

Figura 8. Co-variance diagram (RA/ C_{40}). The graph shows that the samples are grouped into two types: red, indicating a predominance of low values, and blue, indicating a predominance of higher values of the C_{40}).

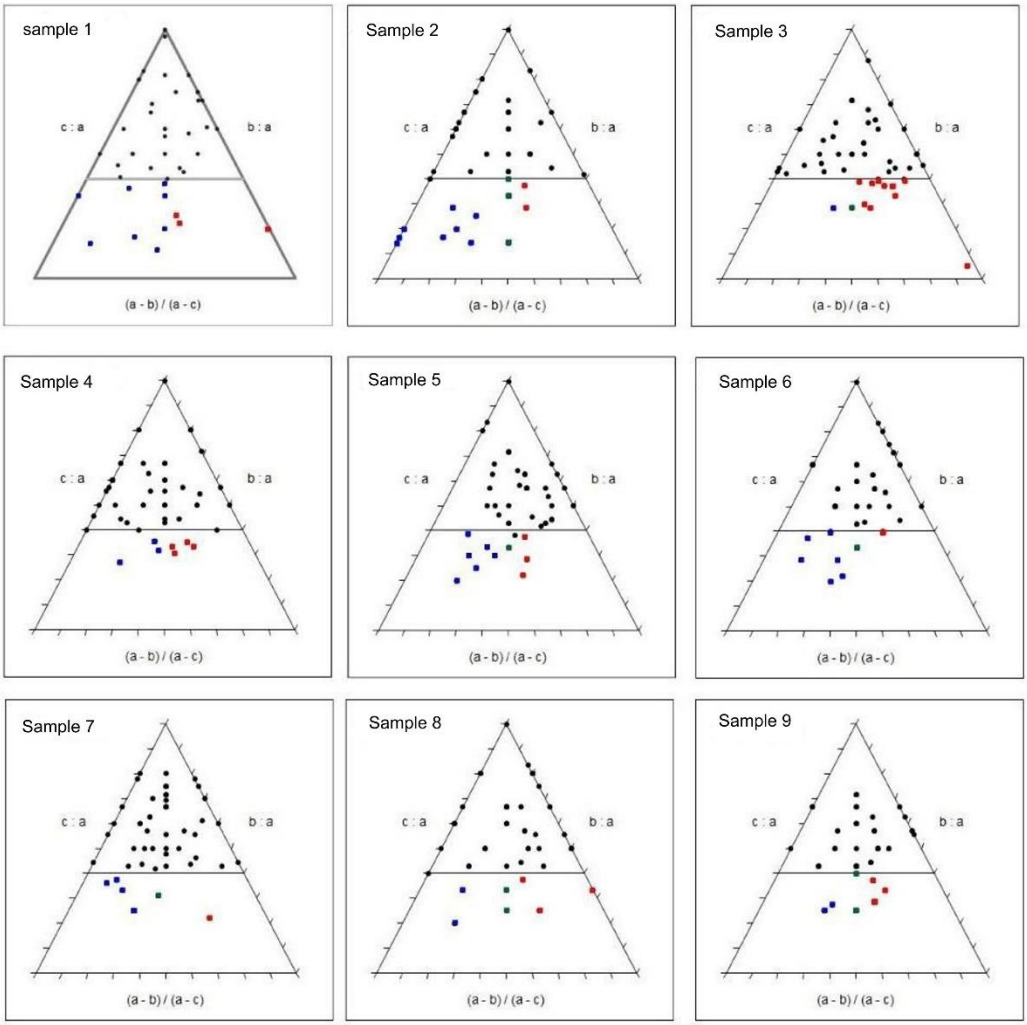

Figure 9. Ternary plots. The straight line indicates the 0.4 threshold for c:a and b:a ratios. Black grains above this line are positioned in the upper part of the diagram, indicating greater form (blocky or cubic shapes); blue grains toward the lower left corner are flattened (disk-shaped); and red grains toward the lower right corner are elongated (major axis > intermediate axis). Intermediate grains are shown in green.

4.2 Geomorphological Mapping of Glacial Landforms

The geomorphological mapping made it possible to identify and spatialize depositional and erosional landforms, contributing to the understanding of proximal and distal processes along the current glacial margin. In the proglacial areas of the Baranowski and Windy glaciers (Figures 10A and 10B), depositional landforms were identified that reveal past glacial characteristics, such as former glacier margin positions, paleo-ice flow directions, and basal thermal regimes, among others. The geomorphological mapping revealed various landforms, including moraines (lateral, frontal, and latero-frontal), some of which extend into the sea, as well as lakes, lagoons, and meltwater channels. Eskers were also identified, along with erosional features such as nunataks and volcanic morphostructures.

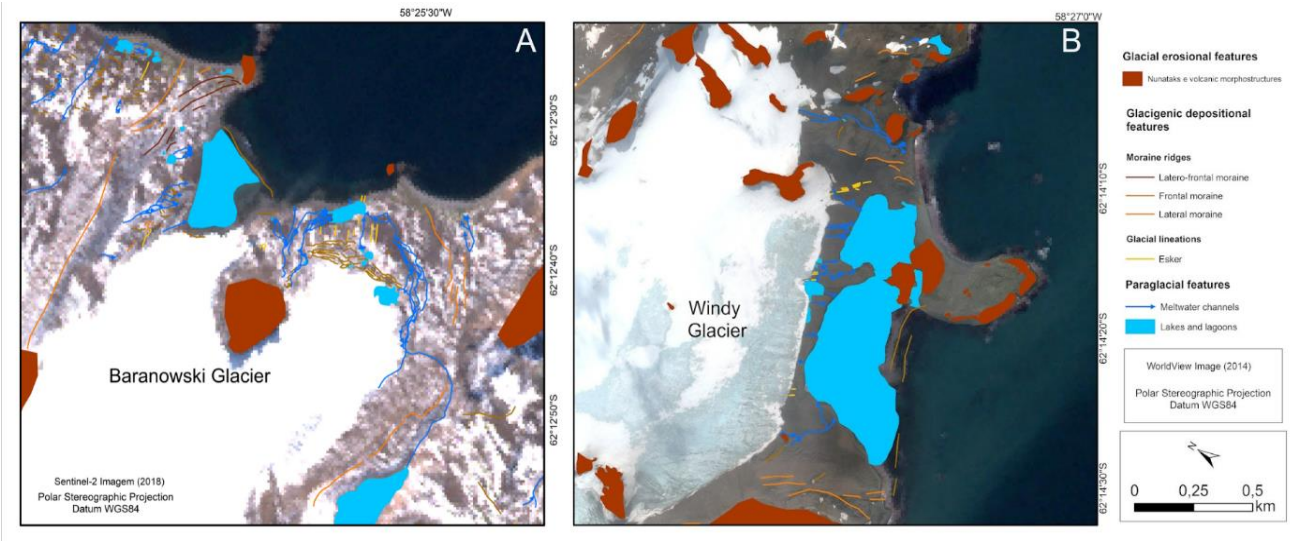

Figure 10. Geomorphological map of glacial landforms in the proglacial area. A.Baranowski Glacier. Satellite image used for this map: Sentinel-2, 2018. B. Windy Glacier. Satellite image used for this map: WorldView-2, March 2014.

5. Discussões

5.1 Associação entre processos e geoformas dos ambientes deposicionais proglaciais

Landforms transverse to the ice flow and prominent in the proglacial sector were interpreted as moraines. Moraines are formed by the direct deposition of glacial material at the frontal margin and record the former positions of glacial fronts (BENNET; GLASSER, 1996). The largest moraine ridges indicate periods of prolonged glacial stabilization and reduced flow velocity (OTTESEN; DOWDESWELL, 2009; BRINKERHOFF et al., 2017). Samples 8 and 9, due to their field-observed location (in contact with the ice) and their slightly arched shape perpendicular to the glacial flow, were interpreted as a recessional frontal moraine (Figures 4B and 4E).

Latero-frontal moraines were also identified in the study area. This depositional feature forms both laterally and frontally along the glacier margin (Figures 4B and 4F). These external moraine ridges represent the glacier's maximum advance during a cooling event that occurred in the early 2000s, as recorded by Turner et al. (2016). Thus, they mark a phase of glacial front stabilization followed by subsequent retreat.

A depositional feature with a distinct spatial configuration was identified, as it is positioned laterally to the Baranowski (Figure 4G) and Windy Glaciers. This landform records the lateral extent of the glacier and its former thickness (BENNET; GLASSER, 1996). Samples were collected from the lateral moraines of Windy (sample 8) and Dobrowolski Glaciers.

An esker was identified on the lateral margin of the Baranowski Glacier, in contact with the ice (sample 1 and Figure 4H). Similar landforms were also observed in contact with and in proximity to the front of the Windy Glacier (Figure 10B). In the study area, eskers were recognized by their sinuous shape; some are well-preserved and measure up to 97 m in length (sample 1). Most of the eskers identified have been situated on ice-free ground for a longer time (ROSA et al. 2011; DĄBSKI et al., 2020). At the Ecology Glacier, Rosa et al. (2013) identified an esker proximal to the glacial front, in contact with the Ecology Lagoon. This feature indicates a wet basal thermal regime and reveals the direction of the glacial flow (BENN; EVANS, 2010).

Additionally, elongated and linear forms smaller than the eskers identified in these same glaciers were observed. In the study area, there are flutings ranging from only a few meters in length—having been reworked and therefore losing their continuity—to flutings reaching up to 33 m, all of which are detached from the glacier. These represent subglacial deformation occurring within cavities that develop downstream of elongated, polished, and asymmetric blocks (stoss and lee), as described by Rosa et al. (2011). The flutings, located downstream of stoss-lee blocks, exhibit asymmetry and indicate glaciers with high velocities and relatively thin ice (GLASSER; BENNET, 2004). These flutings are elongated depositional landforms, parallel to the glacial flow, found

subglacially, and signal that the glacier has a wet basal thermal regime, reduced thickness, and a well-defined flow direction (GLASSER; BENNET, 2004).

Lodgement and subglacial till deposits consist of poorly sorted sediments, which may be stratified or massive. Interpreting the associations of these facies is essential for distinguishing the processes and environments—or the sequence of events (retreat, increased melting, advance) (GLASSER; BENNET, 2004). Basal till is characterized as multimodal (HOEY, 2004), and studies show that it commonly contains polished and striated grains, along with low RA and C_{40} indices (BENN, 2004). Annual changes or events can be indicated either by an erosive contact in the boundary layer of stratified sediments or by a transition from a laminated depositional environment (marginal to the ice with seasonal variations, subglacial flow, or meltwater action) to a massive deposit (lodgement till or subglacial deformation). An advance of the glacial margin over a succession of proglacial fans or deltas causes subglacial deformation of the sediments (BENN; EVANS, 2004).

5.2 Indicativos do tipo de transporte sedimentar (ativo ou passivo)

The sediments in the moraines are marked by poorly sorted granulometry and a bimodal/multimodal distribution. Most samples associated with these landforms exhibit high RA values and low C_{40} values, with grains that are angular to very angular. Sample 8, collected from a recessional moraine (Figure 5A) in contact with the Baranowski Glacier, comprises 54% gravel and 46% sand, with the fine sediments likely transported by water (Table 3). The sedimentary morphology of different depositional environments varies according to their erosion, transport, and deposition histories (BENN, 2004). Their multimodal distribution is typical of active transport (BENN; EVANS, 2010). A low C_{40} index suggests active subglacial transport with grains that have been significantly modified during transit, adopting a more spherical shape.

Sample 9 was collected near a drainage channel adjacent to the current front of the Baranowski Glacier; its sediments are influenced by tidal oscillations, which contribute to their reworking and remobilization. The marginal zones of the glaciers tend to contain coarse sediments, as they are proximal to the source areas (TRUSEL et al., 2010). Samples 6 and 7 share similar characteristics, with the RA/ C_{40} covariance indicating a mix of transport modes and possibly a mixture of lithologies.

Regarding the sedimentary characteristics of samples associated with subglacial forms, there is generally greater grain sorting than in other samples. Samples 1 and 5 share similarities by having low C_{40} values and a significant proportion of angular to subrounded grains, indicative of active subglacial transport (abrasion, fragmentation, and polishing) under conditions of high transport energy and the presence of subglacial meltwater.

Sample 1, collected in the proglacial area of the Windy Glacier on a high, distal plain perpendicular to the glacier front, exhibits the granulometric distribution typical of subglacially transported sediments. These sediments undergo processes such as abrasion and fragmentation, which generate numerous fine particles and cause grain quarrying (BENN; EVANS, 2010). The active subglacial transport is confirmed by the low C_{40} index and the presence of grains that have been notably modified during transport, ranging from subrounded to angular. In the study area, flutings are recognized by having better-sorted sediments than those found in the moraines, displaying low C_{40} values, rounded grains, and striations. This deposit may be reworked, with its fine sediment fraction being transported to areas distal to the current glacier front.

Sample 5 has a low C_{40} index (22%), evidencing subglacial transport and grains that have been significantly modified during active transport, adopting a more spherical shape. The low or absent presence of fine-grained deposits suggests that these have likely been transported by meltwater to other locations, leaving predominantly larger grains.

The analysis of morphoscopic and granulometric characteristics allowed us to infer the genesis (subglacial, englacial, and supraglacial) of the glaciogenic sediments. The sedimentary characteristics of flutings, eskers, and moraine deposits have been described for other proglacial environments on the same island and form the basis for interpreting these landforms and validating the generated mappings. According to Kreczmer *et al*. (2021), Perondi, Rosa and Vieira (2019) and Perondi e*t al.* (2023), these landforms have not been recorded in sedimentary studies yet. Studying the relationship between local geomorphology and sedimentation processes was important because it provided insights into relict processes.

6. Final considerations

Baranowski Glaciers reveal a diversity of depositional and erosional processes associated with glacial dynamics. Depositional features such as moraines, eskers, and flutings were identified, and most samples exhibit striated grains, suggesting that they are glaciogenic deposits. The differences in granulometric and morphoscopic characteristics among the samples demonstrate a direct relationship between the processes of transport, deposition, and erosion, as well as the influence of the glaciers' wet basal thermal regime.

Active subglacial transport with high transport energy and the presence of subglacial meltwater was identified based on the sedimentary characteristics of samples from the proglacial areas of the Windy and Baranowski Glaciers. However, in general, the samples collected near the Baranowski Glacier show a higher degree of grain reworking during glacial transport. Regarding the sampling in the proglacial area of the Windy Glacier, it is recommended to increase the sample size in areas that became ice-free prior to the 1970s, and also to sample the lateral moraine, in order to compare processes and sedimentary characteristics that might indicate changes in glacial processes and the presence of sediments unmodified by weathering.

Precipitation and atmospheric temperature are fundamental elements that condition the behavior of glaciers over time, influencing their advance, retreat, and the duration of their stability. Prolonged periods of frontal stabilization can be better understood through future studies on the chronology of deposits, such as the more extensive and prominent lateral moraines in the study area. It is important to expand the dating of sedimentary records in Admiralty Bay in order to more precisely characterize fluctuations of glacial fronts prior to the 1950s.

Recessional frontal moraines provide evidence of periods of glacial front stabilization followed by retreat, revealing how glaciers respond to variations in atmospheric temperature. Both glaciers analyzed exhibit a proglacial environment with various glacial depositional features, in addition to having undergone significant retreat over recent decades. The recent reduction in glacier thickness is evidenced by the presence of smaller, or even absent, moraine banks in the marginal ice environment, especially in the case of the Windy Glacier.

Furthermore, as glaciers terminating in a terrestrial marginal environment lose area, new ice-free areas are forming, accompanied by the emergence of distinct environmental dynamics and configurations in a sector highly susceptible to paraglacial activity. Thus, monitoring the transformations in these landforms and adjacent sectors is essential for understanding the ongoing geomorphological and hydrological processes.

Future work could focus on spatially delineating mesoscale depositional landforms using data from other studies and high-spatial-resolution images, with the aim of deepening our understanding of the processes operating in the proximal and distal portions of the current glacial margin.

Author's contributions: Conception, Cl.P. and K.K.R.; methodology, Cl.P., K.K.R.; formal analysis, Cl.P. and K.K.R.; data preparation, Cl.P., K.K.R., L.F.V., Ca.P. N.P., S.G..; article writing, Cl.P., K.K.R., L.FV., Ca.P.; revision, Cl.P., K.K.R., L.FV., Ca.P., R.V. e J.C.S. All authors have read and agreed with the published version of the manuscript".

Funding: National Council for Scientific and Technological Development (CNPq) for Project 465680/2014-3 (INCT Criosfera), and Research Support Foundation of the State of Rio Grande do Sul (FAPERGS).

Acknowledgments: We thank the National Council for Scientific and Technological Development (CNPq), Coordination for the Improvement of Higher Education Personnel (CAPES), Brazilian Antarctic Program (PROANTAR), and Research Support of the State of Rio Grande do Sul (FAPERGS) for financial support.

Conflict of interest: The authors declare no conflict of interest.

References

1. ANGIEL, P.J.; DĄBSKI, M. Lichenometric ages of the little ice age moraines on King George Island and of the last volcanic activity on Penguin Island (West Antarctica). **Geografiska Annaler: Series A, Physical Geography**, v. 94, n. 3, p. 395–412, 2012. DOI: 10.1111/j.1468-0459.2012.00460.x
2. ASSINE, M.L.; VESELY, F.F. Ambientes Glaciais. In: PEDREIRA DA SILVA, A.J.; ARAGÃO, A.N.F.; MAGALHÃES, A.J.C. (Eds.). **Ambientes de Sedimentação Siliciclástica do Brasil**. São Paulo: Ed. Beca, p. 24-51, 2008.
3. ARNDT, J.E.; EVANS, J. Glacial lineations and recessional moraines on the continental shelf of NE Greenland. **Geological Society Memoirs**, v. 46, p. 263-264, 2016. DOI: 10.1144/M46.81

4. BALLANTYNE, C.K. Glacial landforms, ice sheets: Trimlines and palaeonunataks. **Encyclopedia of Quaternary Science**, p. 892-903, 2007. DOI: 10.1016/B0-44-452747-8/00100-9.
5. BALLANTYNE, C.K. Paraglacial geomorphology. **Quaternary Science Reviews**, v. 21(18-19), p. 1935-2017, 2002. DOI: 10.1016/S0277-3791(02)00005-7
6. BARRIOPEDRO, D.; TRIGO, R. M.; ALBERT, J.; OLIVA, M. Climate warming amplified the 2020 record-breaking heatwave in the Antarctic Peninsula. **Communications Earth & Environment**, v. 3(1), p. 1-9, 2022. DOI: 10.1038/s43247-022-00450-5
7. BATCHELOR, C.L.; DOWDESWELL, J.A.; RIGNOT, E. Submarine landforms reveal varying rates and styles of deglaciation in North-West Greenland fjords. **Marine Geology**, v. 402, p. 60-80, 2018. DOI: 10.1016/j.margeo.2017.08.003
8. BENN, D.I.; BALLANTYNE, C.K. Reconstructing the transport history of glaciogenic sediments – a new approach based on the covariance of clast form indices. **Sedimentary Geology**, v. 91, p. 215-227, 1994. DOI: 10.1016/0037-0738(94)90130-9
9. BENN, D.I. 2004. Clast morphology. In: **A Practical Guide to the Study of Glacial Sediments**. 1º edition, Quaternary Research Association, London, 375 p.
10. BENN, D.I.; EVANS, D.J.A. **Glaciers and glaciation**. 2ª ed. London: Hodder Education, 2010. 802p.
11. BENNETT M.R.; GLASSER, N.F. **Glacial geology – ice sheets and landforms**. England: John Wiley & Sons Ltd. 1996. 364 p.
12. BIRKENMAJER, K. Geology of Admiralty Bay, King George Island (South Shetland Islands) — An outline. **Polish Polar Research**, v. 1, n. 1, p. 29-54, 1980.
13. BREMER, U.F. **Morfologia e bacias de drenagem da cobertura de gelo da ilha Rei George, Antártica**. Dissertação (Sensoriamento Remoto) - Universidade Federal do Rio Grande do Sul. 117p. 1998.
14. BREMER, U.F.; ARIGONY-NETO, J.; SIMÕES, J. C. Teledetecção de mudanças nas bacias de drenagem do gelo da ilha Rei George, Shetlands do Sul, Antártica, entre 1956 e 2000. **Pesquisa Antártica Brasileira**, v. 4, p. 37-48, 2004.
15. BRENNAND, T. A. (2004). Glacifluvial. In: GOUDIE, A. S. (Ed.) Encyclopedia of geomorphology. London: Routledge, v. 1, p. 459-465.
16. BRINKERHOFF, D.; TRUFFER, M.; ASCHWANDEN, A. Sediment transport drives tidewater glacier periodicity. **Nature Communications**, v.8, n. 1, p. 90–98, 2017. DOI: 10.1038/s41467-017-00095-5
17. CASALBORE, D. Volcanic Islands and Seamounts. In: MICALLEF, A.; KRASTEL, S.; SAVINI, A. (Eds.). **Submarine Geomorphology**. Springer Geology, p. 333-347, 2018.
18. CAREY, S. Volcaniclastic sedimentation around island arcs. In: SIGURDSSON H. (Ed). **Encyclopedia of volcanoes**. Academic Press, San Diego, p. 627–642, 2000.
19. DĄBSKI, M.; ZMARZ, A.; RODZEWICZ, M.; KORCZAK-ABSHIRE, M.; KARSZNIA, I.; LACH, K.M.; RACHLEWICZ, G.; CHWEDORZEWSKA, K.J. Mapping Glacier Forelands Based on UAV BVLOS Operation in Antarctica. **Remote Sensing**, v. 12, n. 4, 2020. DOI: 10.3390/rs12040630
20. DING, Y.; MU, C.; WU, T.; HU, G.; ZOU, D.; WANG, D.; LI, W.; WU, X. Increasing cryospheric hazards in a warming climate. **Earth-Science Reviews**, 213, 103500, 2021. DOI: 10.1016/j.earscirev.2020.103500
21. DIOLAIUTI, G.; SMIRAGLIA, C. Changing glaciers in a changing climate: How vanishing geomorphosites have been driving deep changes in mountain landscapes and environments. **Geomorphologie: Relief, Processes, Environment**, v. 16, n. 2, p. 131-152, 2010. DOI: 10.4000/geomorphologie.7882
22. DIONNE, J.C. 1987. Tadpole rock (rocdrumlin): a glacial streamline moulded form. *In*: Menzies, J.; Rose, J. (eds), **Drumlin Symposium**. Balkema, Rotterdam, 149–59.
23. DOWDESWELL, J.A.; OTTESEN, D.; RISE L. Flow-switching and large-scale deposition by ice streams draining former ice sheets. **Geology**, v. 34, p. 313–316, 2006. DOI: 10.1130/G22253.1
24. DOWDESWELL, J.A.; OTTESEN, D.; NOORMETS, R. Submarine slides from the walls of Smeerenburgfjorden, NW Svalbard. In: DOWDESWELL, J.A.; CANALS, M.; JAKOBSSON, M.; TODD, B.J.; DOWDESWELL, E.K.; HOGAN, K.A. (Eds.). **Atlas of Submarine Glacial Landforms: Modern, Quaternary and Ancient**. p. 105–106, 2016.
25. DREWRY, D. J. **Glacial Geologic Processes**. 1ª ed. Edward Arnold, London, 1986.

26. EIDAM, E.F.; SUTHERLAND, D.A.; DUNCAN, D.; KIENHOLZ, C.; AMUNDSON, J.M.; MOTYKA, R.J. Morainal bank evolution and impact on terminus dynamics during a tidewater glacier stillstand. **Journal of Geophysical Research Earth Surface**. 2020. DOI: 10.1029/2019JF005359
27. EVANS, D.J.A. **Glacial landsystems**. 1ª ed. London: Hodder Arnold. 2003. 545 p.
28. EVANS, D.J.A.; BENN, D.I. Facies description and the logging of sedimentary exposures. In: EVANS, D.J.A.; BENN, D.I. 2004. **A Practical Guide to the Study of Glacial Sediments**. 1º edition, Quaternary Research Association, London, 375 p. 2004.
29. EVANS, J.A.; PUDSEY, C.J.; Ó COFAIGH, C.; MORRIS, P.; DOMACK, E. Late Quaternary glacial history, flow dynamics and sedimentation along the eastern margin of the Antarctic Peninsula Ice Sheet. **Quaternary Science Reviews**, v. 24, p.741–74, 2005. DOI: 10.1016/j.quascirev.2004.10.007
30. FERRON, F.A.; SIMÕES, J.C.; AQUINO, F.E.; SETZER, A.W. Air temperature time series for King George Island, Antarctica. **Pesquisa Antártica Brasileira**, v. 4, p. 155-169, 2004. DOI: 10.31789/pab.v4n1.012
31. FOLK, R.L; WARD, W.C. Petrol Brazos River bar: a study in the significance of grain size parameters. **Journal Sedimentology**, v.3, n. 27, p.3-26, 1957.
32. HAMBREY, M. **Glacial Environments**. London: CRC Press. 1994. 304 p.
33. HANÁČEK, M.; NÝVLT, D.; FLAŠAR, J.; STACKE, V.; MIDA, P.; LEHEJČEK, J.; TÓTHOVÁ, G.; BŘEŽNÝ, M.; PROCHÁZKOVÁ, B.; UX, T.; KŘENOVSKÁ, I. New methods to reconstruct clast transport history in different glacial sedimentary environments: Case study for Old Red sandstone clasts from polythermal Hrbyebreen and Bertilbreen valley glaciers, Central Svalbard. **Czech Polar Reports**, v. 3, n.2, p. 107-12, 2013. DOI: 10.5817/CPR2013-2-13
34. HOEY, T.B. 2004. The size of sedimentary particles In: Evans, D.J. & Benn, D.I. 2004. **A Practical Guide to the Study of Glacial Sediments**. 1º edition, Quaternary Research Association, London, 375 p.
35. HOCK, R.; HUSS, M. Glaciers and climate change. **Climate Change (Third Edition)**, p. 157-176, 2021. DOI: 10.1016/B978-0-12-821575-3.00009-8
36. HOWAT, I. et al. 2022. The Reference Elevation Model of Antarctica – Strips, Version 4.1. Disponível em: https://doi.org/10.7910/DVN/X7NDNY, Harvard Dataverse, V1. Acesso em: 20 de abril de 2024.
37. HUBBARD, B.; GLASSER, N. **Field Techniques in Glaciology and Glacial Geomorphology**. England: John Wiley & Sons Ltd, 412p. 2005.
38. KEJNA, M.; ARAZNY, A.; SOBOTA, I. Climatic change on King George Island in the years 1948 – 2011. **Polish Polar Research**, v. 34, n. 2, p. 213-235, 2013. DOI: 10.2478/popore−2013−0004
39. KNIGHT, P.; PATTERSON, C.J.; WALLER, R.I.; JONES, A.P.; ROBINSON, Z.P. Preservation of basal-ice sediment texture in ice-sheet moraines. **Quaternary Science Review**, v.19, p. 1255-1258, 2000. DOI: 10.1016/S0277-3791(00)00091-3
40. KRAUS A.S.; POBLETE, B.F.; ARRIAGADA C. Dike systems and their volcanic host rocks on King George Island, Antarctica: Implications on the geodynamic history based on a multidisciplinary approach. **Tectonophysics**, v. 495, p. 269–297, 2010. DOI: 10.1016/j.tecto.2010.09.035
41. KRECZMER, K.; DĄBSKI, M.; ZMARZ, A. Terrestrial Signature of a Recently-Tidewater Glacier and Adjacent Periglaciation, Windy Glacier (South Shetland Islands, Antarctic). **Frontiers in Earth Science**, v. 9, 2021. DOI: /10.3389/feart.2021.671985
42. KRUMBEIN, W.C.; PETTIJOHN, F.J. **Manual of Sedimentary Petrography**. D. Appleton-Century, New York, 1938, 549 p.
43. LORENZ, J.; ROSA, K.K.; PETSCH, C.; PERONDI, C.; IDALINO, F.; AUGER, J.; VIEIRA, R.; SIMÕES, J.C. Short-term glacier area changes, glacier geometry dependence, and regional climatic variations forcing, King George Island, Antarctica. **Anais da Academia Brasileira de Ciências**. 2023. DOI: 10.1590/0001-3765202320211627
44. MAGRANI, F**. Caracterização sedimentar glaciomarinha da deglaciação da BA desde o Último Máximo Glacial, arquipélago das Shetlands Do Sul, Antártica**. Dissertação de mestrado. Universidade Federal Fluminense, 198 p. 2014.
45. MATSUOKA, K.; SKOGLUND, A.; ROTH G. Quantarctica [Dataset]. Norwegian Polar Institute. 2018.
46. MICALLEF, A.; KRASTEL, S.; SAVINI, A. (Eds.). **Submarine geomorphology**. Springer Geology. 2018. 552p.

47. NAPIERALSKI, J.; HARBOR, J.; LI, Y. Glacial geomorphology and geographic information systems. **Earth Science Review**, v. 85, n. 1-2, 2007. DOI: 10.1016/j.earscirev.2007.06.003.
48. NITSCHE, F.O.; GOHL, K.; LARTER, R.; HILLENBRAND, C.D.; KUHN, G.; SMITH, J.; JACOBS, S.; ANDERSON, J.; JAKOBSSON, M. Paleo ice flow and subglacial meltwater dynamics in Pine Island Bay, West Antarctica. **The Cryosphere**, v. 6, p. 4267–4304, 2012. DOI: 10.5194/tc-7-249-2013
49. OLIVEIRA, M.G. **Evolução de lagos marginais ao gelo em resposta à retração de geleiras nas ilhas Nelson e Rei George, Antártica Marítima**. Dissertação de mestrado. Universidade Federal do Rio Grande do Sul. Porto Alegre. 105p. 2020.
50. OTTESEN, D.; DOWDESWELL, J.A. An inter-ice stream glaciated margin: submarine landforms and a geomorphic model based on marine-geophysical data from Svalbard. **GSA Bullettin,** v. 121, n. 11-12, p.1647–1665, 2009. DOI: 10.1130/B26467.1
51. PATTERSON, C.J.; HOOKE, R.B. Physical environment of drumlin formation. **Journal of Glaciology**, v. 41, n. 137. 30–8. 1996. DOI: 10.3189/S0022143000017731
52. PERONDI, C.; ROSA, K.K.; VIEIRA, R. Caracterização geomorfológica das áreas livres de gelo na margem leste do campo de gelo Warszawa, ilha Rei George, Antártica Marítima. **Revista Brasileira de Geomorfologia**, v. 20, n. 2, 2019. DOI: 10.20502/rbg.v20i2.1433
53. PERONDI, C.; ROSA, K.K.; MAGRANI, F.; PETSCH, C.; VIEIRA, R.; AYRES NETO, A.; SIMÕES, J.C. Paleoglaciological reconstruction and geomorphological mapping of Dobrowolski Glacier, King George Island, Antarctica. **Revista Brasileira de Geomorfologia**, 2023. DOI: 10.20502/rbg.v24i3.2425
54. PETSCH, C.; PERONDI, C.; ROSA, K.K.; VELHO, L.F.; TRENTIN, R.; VIEIRA, R. Identificação de geoformas glaciais por análise visual e por análise de relevo: um comparativo entre sensores orbitais e VANT. **14°SINAGEO**, Corumbá-MS. 2023.
55. POST, A.; MOTYKA, R.J. Taku and LeConte glaciers, Alaska: Calving-speed control of late-Holocene asynchronous advances and retreats. **Physical Geography**, v. 16 n. 1, p. 59–82, 1995. DOI: 10.1080/02723646.1995.10642543
56. ROSA, K.K.; VIEIRA, R.; FERNANDEZ, G.; SIMÕES, F.; SIMÕES, J.C. Glacial landforms and glaciological processes of the temperate Wanda Glacier, South Shetlands. **Investigaciones Geográficas**, v. 43, p. 3-16, 2011.
57. ROSA, K.K.; VIEIRA, R.; MENDES, J.R.C.; SOUZA, J.R.; SIMÕES, J.C. Compilation of geomorphological map for reconstructing the deglaciation of ice-free areas in the Martel inlet, King George Island, Antarctic. **Revista Brasileira de Geomorfologia**, v. 14, p. 181-187, 2013. DOI: 10.20502/rbg.v14i2.324
58. ROSA, K.K.; PERONDI, C.; VEETTIL, B.K.; AUGER, J.D.; SIMÕES, J.C. Contrasting responses of land-terminating glaciers to recent climate variations in King George Island, Antarctica. **Antarctic Science**, v. 32, n. 5, p. 398–407, 2020. DOI: 10.1017/S0954102020000279
59. RÜCKAMP, M.; BRAUN, M.; SUCKRO, S.; BLINDOW, N. Observed glacial changes on the King George Island ice cap, Antarctica, in the last decade. **Global and Planetary Change**, v. 79, p. 99–109, 2011. DOI: 10.1016/j.gloplacha.2011.06.009
60. SETZER, A.W.O.; FRANCELINO, M.R.; SCHAEFER, C.E.G.R.; COSTA, L.V.; BREMER, U.F. Regime climático na baía do Almirantado: relações com o ecossistema terrestre. In: SCHAEFER, C. (Ed.). **Ecossistemas costeiros e monitoramento ambiental da Antártica Marítima.** Minas Gerais: Viçosa, p. 1–13, 2004.
61. SHAHGEDANOVA, M. Climate change and melting glaciers. **The Impacts of Climate Change**, p. 53-84, 2021. DOI: 10.1016/B978-0-12-822373-4.00007-0
62. SIEGERT, M.; ATKINSON, A.; BANWELL, A.; BRANDON, M.; COVEY, P.; DAVIES, B.; DOWNIE, R.; EDWARDS, T.; HUBBARD, B.; MARSHALL, G.; ROJELL, J.; RUMBLE, J.; STROEVE, J.; VAUGHAN, D. The Antarctic Peninsula Under a 1.5°C Global Warming Scenario. **Frontiers in Environmental Science**, v. 28, 2019. DOI: 10.3389/fenvs.2019.00102
63. SILVA, A.B.; ARIGONY-NETO, J.; BICCA, C.E. Caracterização geomorfológica das geleiras da Península Antártica. **Revista Brasileira de Geomorfologia**, v. 20, n. 3, 2019. DOI: 10.20502/rbg.v20i3.1547
64. STEARNS, L.A.; HAMILTON, G.S.; VAN DER VEEN, C.J.; FINNEGAN, D.C.; O'NEEL, S.; SCHEICK, J. B.; LAWSON, D.E. Glaciological and marine geological controls on terminus dynamics of Hubbard Glacier, southeast Alaska. **Journal of Geophysical Research: Earth Surface**, v. 120, p. 1065–1081, 2015. DOI: 10.1002/2014JF003341

65. STREUFF, K.; FORWICK, M.; SZCZUCINSKI, W. ANDREASSEN. K.; Ó COFAIGH, C. Submarine landform assemblages and sedimentary processes related to glacier surging in Kongsfjorden, Svalbard. **ArKtos**, v. 1, n. 14, 2015. DOI: 10.1007/s41063-015-0003-y
66. SUGDEN, D. E.; JOHN B. S. **Glaciers and Landscape**: A Geomorphological Approach. London; New York: Editora Edward Arnold, 2ª ed. 1984. 376 p.
67. SUGDEN, D.E.; BALCO, G.; COWDERY, S. G.; STONE, J. O.; SASS, L. C. Selective glacial erosion and weathering zones in the coastal mountains of Marie Byrd Land, Antarctica. **Geomorphology**, 67, 317–34, 2005. DOI: 10.1016/j.geomorph.2004.10.007
68. SUGDEN, D.E.; BENTLEY, M.J.; Ó COFAIGH, O. Geological and geomorphological insights into Antarctic ice sheet evolution. **Philosophical Transactions of the Royal Society**, v. 364, p.1607–1625, 2006. DOI: 10.1098/rsta.2006.1791
69. TanDEM-X. Digital Elevation Model (DEM). Global, 12m. (n.d.). Disponível em: http://data.europa.eu/88u/dataset/5eecdf4c-de57-4624-99e9-60086b032aea Acesso em 27 de abril de 2025.
70. TOKARSKI, A.K. Structural events in the South Shetland Islands (Antarctica). III. Barton Horst, King George Island. **Studia Geologica Polonica**, v. 90, p. 7-38. 1987.
71. TRUSEL, L.D.; POWELL, R.D.; CUMPSTON, R.M.; BRIGHAM-GRETTE, J. Modern Glacimarine Processes and Potential Future Behaviour of Kronebreen and Kongsvegen Polythermal Tidewater Glaciers, Kongsfjorden, Svalbard. In: HOWE, J.A.; AUSTIN, W.E.N.; FORWICK, M.; PAETZEL, M. (Eds.). **Fjord Systems and Archives**. Geological Society Special Publications. n. 344. p. 89–102. London. 2010.
72. TURNER, J.; LU, H.; WHITE, I.; KING, J.C.; PHILLIPS, T.; HOSKING, J.S.; BRACEGIRDLE, T.J.; MARSHALL, G.J.; MULVANEY, R.; DEB, P. Absence of 21st century warming on Antarctic Peninsula consistent with natural variability. **Nature**, v. 535, p. 411–415, 2016. DOI: 10.1038/nature18645
73. WENTWORTH, C. K. A 1922. Scale of Grade and Class Terms for Clastic Sediments, **The Journal of Geology**, v. 30, n. 5, p. 377-392.
74. WÖLFL, A.C.; WITTENBERG, N.; FELDENS, P.; HASS, H.C.; BETZLER, C.; KUHN, G. Submarine landforms related to glacier retreat in a shallow Antarctic fjord. **Antarctic Science**, v. 28, p. 475–486, 2016. DOI: 10.1017/S0954102016000262